Int. J. Heat Mass Transfer. Vol. 32, No. 3, pp. 617–620, 1989
Printed in Great Britain

0017–9310/89 $3.00 + 0.00

Transient forced and natural convection heat transfer about a vertical cylinder in a porous medium

SHIGEO KIMURA
Government Industrial Research Institute, Tohoku, 4-2-1 Nigatake, Sendai 983, Japan

(*Received* 11 *April* 1988 *and in final form* 18 *July* 1988)

1. INTRODUCTION

TRANSIENT heat transfer from a vertical cylinder placed in a saturated porous medium is considered. It is assumed that flows about the cylinder are driven either by the imposed pressure drop in the vertical direction or by fluid density variation due to the temperature difference in the radial direction, but not by both of them simultaneously. When the surface of the cylinder is raised to a higher temperature than the surrounding medium and maintained at that temperature thereafter, heat from the cylinder will uniformly diffuse in the radial direction at an early time. As the thermal layer grows, however, the vertically convecting flows start to give measurable effects on the heat transfer rate and eventually lead to a steady state defined by vigorous convection [1]. The purpose of this note is to describe the transient heat transfer characteristics over a time period extending from the early conductive to the final convective steady state in the presence of either forced or natural convection. This note shows that the transient heat transfer for both forced and natural convection may be expressed in a unified manner, with a single parameter representing the curvature effect of the cylinder surface.

The associated steady-state problems have been studied in refs. [2, 3] for forced convection and by Minkowycz and Cheng [4] for natural convection. Nakayama and Koyama [5] showed the applicability of a general transformation technique developed by Merkin [6] for describing mixed convection heat transfer about two-dimensional and axisymmetric bodies of arbitrary shape. However, a few cases are known on the time-dependent heat transfer by external flows in porous media, such as natural convection about a point heat source [7] and over a finite horizontal plate [8]. Understanding the transient characteristics in porous media is important in view of their slow evolution processes to steady states. It is also worth mentioning that the transient process has a potential application to measurement for thermal properties of soil and rock formation as well as for underground water velocity.

2. MATHEMATICAL FORMULATION AND SOLUTION

Assuming axisymmetric flows and temperature fields, constant properties except the density variation due to the temperature gradient and the validity of Darcy's law, the nondimensional conservation equations of mass, momentum and energy are

$$\frac{\partial^2\psi}{\partial r^2} - \frac{\partial\psi}{r\partial r} + \frac{\partial^2\psi}{\partial z^2} = \frac{Ra}{Pe}\frac{\partial\theta}{\partial r} \tag{1}$$

$$\frac{\partial\theta}{\partial\tau} + \frac{Pe}{r}\frac{\partial(\theta,\psi)}{\partial(r,z)} = \nabla^2\theta \tag{2}$$

where the mass conservation equation has already been eliminated by introducing the stream function ψ. The length, time, velocity and temperature are scaled by the cylinder radius a, the diffusion time $\sigma a^2/\alpha$, the vertical velocity U_∞ and the temperature difference ΔT, respectively. The validity of Darcy's law is guaranteed when the Reynolds number based on the pore size is smaller than unity. This condition is normally satisfied by underground water flows. The schematic diagram and the coordinate system are shown in Fig. 1. The Rayleigh and Peclet numbers are defined by

$$Ra = \frac{g\beta Ka\Delta T}{\alpha\nu} \tag{3}$$

$$Pe = \frac{U_\infty a}{\alpha}. \tag{4}$$

In the following analysis one only considers either forced convection ($Ra = 0$) or natural convection ($Pe = 1$). The boundary conditions for forced convection are

$$\begin{aligned} &\theta = 1, \quad \psi = 0 && \text{on } r = 1\\ &\theta = 0, \quad \psi = (R-1)^2/2 && \text{on } r = R\\ &\theta = 0, \quad \psi = (r-1)^2/2 && \text{on } z = -Z\\ &\theta_z = 0, \quad \psi_z = 0 && \text{on } z = H \end{aligned} \tag{5}$$

where R, Z and H are arbitrary large numbers which define the size of the computational field. For natural convection the bottom boundary conditions are replaced so that flows and temperatures there develop themselves as time integration proceeds

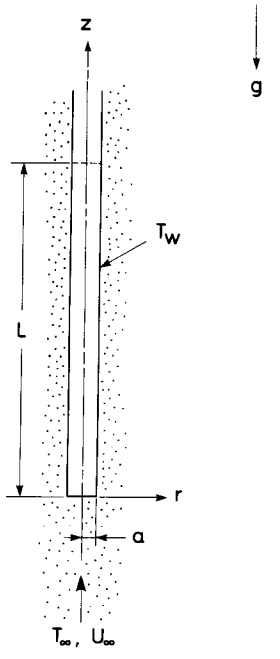

FIG. 1. Schematic diagram of a vertical cylinder in a porous medium and the coordinate system.

NOMENCLATURE

a	cylinder radius
c	specific heat
C	function of ξ
g	gravitational acceleration
h	average heat transfer coefficient
H	non-dimensional cylinder height, L/a
k_e	effective thermal conductivity, $k_f\phi+(1-\phi)k_s$
K	permeability of porous matrix
L	cylinder height
Nu	Nusselt number, hL/k_e
Pe	Peclet number
r	coordinate of radial direction
Δr	grid space in radial direction
R	constant indicating a radial boundary
Ra	Rayleigh number
t	time
T	temperature
ΔT	temperature difference, T_w-T_∞
U	fluid velocity in forced convection
x	transformed radial coordinate
z	vertical coordinate
Z	constant defining a bottom boundary.

Greek symbols

α	thermal diffusivity of a saturated porous medium, $k_e/(\rho c)_f$
β	thermal expansion coefficient
ζ	non-dimensional parameter defined by equation (10)
θ	non-dimensional temperature
ν	kinematic viscosity
ξ	non-dimensional parameter defined by equation (9)
ρ	fluid density
σ	thermal capacity ratio, $((\rho c)_f\phi+(\rho c)_s(1-\phi))/(\rho c)_f$
τ	non-dimensional time, $t\alpha/\sigma a^2$
ϕ	porosity
ψ	non-dimensional stream function.

Subscripts

c	transition to convective steady state
f	saturated fluid
L	characteristic dimension
s	porous matrix
w	conditions at cylinder wall
∞	conditions at infinity.

$$\begin{aligned}&\theta=1, \quad \psi=0 \quad \text{on } r=1\\ &\theta=0, \quad \psi=0 \quad \text{on } r=R\\ &\theta_z=0, \quad \psi_z=0 \quad \text{on } z=-Z\\ &\theta_z=0, \quad \psi_z=0 \quad \text{on } z=H.\end{aligned} \tag{6}$$

A sudden rise in the surface temperature at $\tau=0$ serves as an initial condition for both cases.

2.1. *Small time solution*

When τ is small and the thermal layer is still thin, the convective inertia terms in equation (2) are negligibly small relative to the diffusion terms [1]. Therefore, the energy equation is reduced to the transient heat conduction equation, for which one can derive analytical solutions [9]. Considering the fact that the steady-state average Nusselt number over the cylinder height L is scaled by $\sqrt{Pe_L}$ for forced convection and by $\sqrt{Ra_L}$ for natural convection, the dimensionless heat transfer results valid for small τ may be written as

$$\frac{Nu}{\sqrt{Pe_L}}=\zeta\left(\frac{1}{\sqrt{\pi\tau}}+\frac{1}{2}-\frac{1}{4}\sqrt{\left(\frac{\tau}{\pi}\right)}+\frac{\tau}{8}-\cdots\right) \tag{7}$$

$$\frac{Nu}{\sqrt{Ra_L}}=\xi\left(\frac{1}{\sqrt{\pi\tau}}+\frac{1}{2}-\frac{1}{4}\sqrt{\left(\frac{\tau}{\pi}\right)}+\frac{\tau}{8}-\cdots\right) \tag{8}$$

where ζ and ξ measure the surface curvature effects and are defined by

$$\zeta=\frac{L}{a\sqrt{Pe_L}} \tag{9}$$

$$\xi=\frac{L}{a\sqrt{Ra_L}}. \tag{10}$$

2.2. *Large time solution*

At large times the radially conducting heat must be balanced by the vertically convecting one to realize a steady state. Based on boundary layer analysis, the heat transfer results in terms of Nusselt number may be expressed as a function of ζ for forced convection [3] and of ξ for natural convection [4]

$$\frac{Nu}{\sqrt{Pe_L}}=\frac{2}{\sqrt{\pi}}+\frac{1}{2}\zeta-\frac{1}{6\sqrt{\pi}}\zeta^2+\frac{1}{16}\zeta^3-\cdots \tag{11}$$

$$\frac{Nu}{\sqrt{Ra_L}}=2C(\xi). \tag{12}$$

Equation (12) has been deduced from the original work of Minkowycz and Cheng [4], in which the function C is also tabulated up to $\xi=5$.

2.3. *Complete two-dimensional solution*

Finite difference solutions for the complete governing equations with the respective boundary conditions have been sought in order to test the validity of the preceding analyses. In order to provide fine grid spaces in the vicinity of the cylinder surface one makes the following coordinate transformation in the radial direction:

$$x=\ln(r/a). \tag{13}$$

The transformed governing equations were put in finite difference forms using the second upwind method for the convective terms. The time integration was initiated by the sudden rise of the cylinder surface temperature. A typical grid network used for the computation was 80×150. The grid spaces and network systems were slightly varied and optimized for the respective parametric settings. For example, the grid space next to the cylinder surface was varied from $\Delta r=0.1$ to 0.01 depending on the expected boundary layer thickness. A typical convergence criterion used is

$$\text{Max}\,|\theta_{ij}^{k+1}-\theta_{ij}^{k}|\leqslant 10^{-5} \tag{14}$$

where superscripts indicate the order of time integration.

3. RESULTS AND DISCUSSION

Figure 2 shows the average Nusselt numbers for forced convection as a function of time. Two values of $\zeta=0.5$ and 1 are shown in the figure. Solid lines represent Nusselt numbers obtained from equation (7), while dashed lines are obtained from equation (11). Four different combinations of Pe and L/a in the numerical computation are shown with

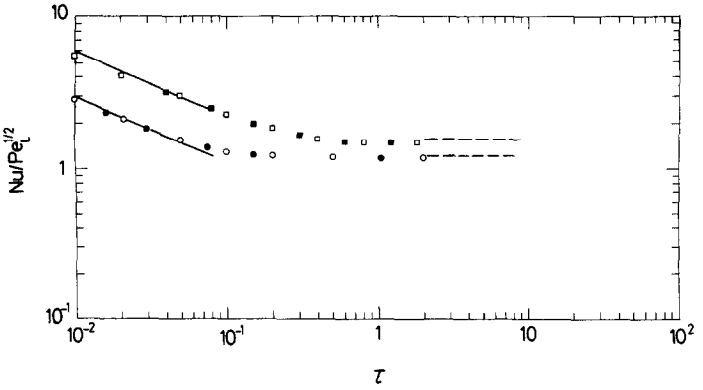

FIG. 2. Transient average Nusselt number for forced convection. Solid and dashed lines are analytical results valid for small and large times, respectively. Various symbols indicate numerical ones: ○, $Pe = 52$ and $H = 13$ ($\zeta = 0.5$); ●, $Pe = 104$ and $H = 26$ ($\zeta = 0.5$); □, $Pe = 10$ and $H = 10$ ($\zeta = 1$); ■, $Pe = 40$ and $H = 40$ ($\zeta = 1$).

various symbols. However, they were chosen in order to yield only two different values of ζ, 0.5 and 1. The numerical results demonstrate that ζ is the proper parameter to correlate the Nusselt number with time in both the transient and steady state. In general, the numerically generated Nusselt numbers at small times agree with the solid lines and at large times they approach the dashed lines. This proves the earlier perception on the transient process. It is also seen that the numerical results tend to underestimate the Nusselt numbers in the range of $\tau \leqslant 0.02$. This is probably due to insufficient resolution of the extremely thin thermal layer; a difficulty typical of numerical solution.

The average Nusselt numbers are shown for natural convection as a function of time in Fig. 3. The meanings of the lines and symbols are the same as those in Fig. 2. The results for $\xi = 1$ and 5 only are shown in the figure. At small times the numerically computed Nusselt numbers agree with the heat conduction solutions, while at large times they gradually approach the values predicted by equation (12). Overall transient characteristics for natural convection closely resemble those found for forced convection.

Another important conclusion from the present study is the time required to reach steady state. A reduction in the time to achieve steady state with increasing ζ and ξ is a common feature between the two systems. One can argue this point based on scaling analysis [10]. The scaling analysis suggests that the time to steady state must be proportional to that for a fluid element to travel over a characteristic distance with a characteristic velocity. In forced convection the statement is equivalent to

$$t_c \sim \frac{L}{U_\infty} \sim \frac{\sigma a^2 L^2/\alpha}{\sigma a^2 Pe_L}. \tag{15}$$

Nondimensionalizing the above equation, one obtains

$$\tau_c \sim \frac{t_c}{\sigma a^2/\alpha} \sim \frac{L^2}{\sigma a^2 Pe_L} \sim \zeta^2. \tag{16}$$

In natural convection, recognizing that the characteristic velocity is

$$U_\infty \sim \frac{\rho g \beta K \Delta T}{\mu} \tag{17}$$

and following the same procedure as before, one obtains the proportionality similar to equation (16)

$$\tau_c \sim \frac{t_c}{\sigma a^2/\alpha} \sim \frac{L^2}{\sigma a^2 Ra_L} \sim \zeta^2. \tag{18}$$

Dependency of τ_c on ζ and ξ is shown in Fig. 4. It is seen that the numerically determined τ_c's for both forced and natural convection are in good agreement with respective straight lines, each of them has a slope of two as proposed by equations (16) and (18). It should be noted here that the τ_c's shown in the figure indicate points when the difference between temporal and steady-state Nusselt numbers fall within 5% in relative magnitude. Since the Nusselt number changes with time become extremely slow toward the steady states, it is often found that the precise points are difficult to determine. Possible errors associated with them are shown in the figure.

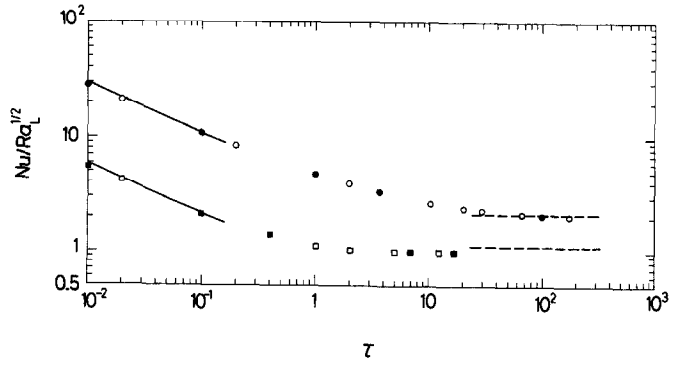

FIG. 3. Transient Nusselt number for natural convection. Lines have the same meanings as those in Fig. 2. Numerical results are indicated by various symbols: ○, $Ra = 2$ and $H = 50$ ($\xi = 5$); ●, $Ra = 4$ and $H = 100$ ($\xi = 5$); □, $Ra = 25$ and $H = 25$ ($\xi = 1$); ■, $Ra = 50$ and $H = 50$ ($\xi = 1$).

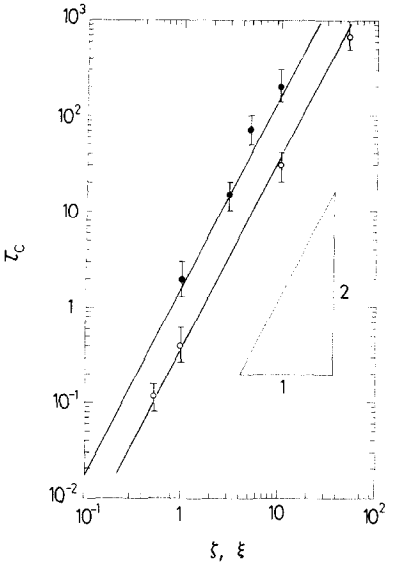

FIG. 4. Non-dimensional time to reach convective steady state as a function of ζ for forced convection (○) and ξ for natural convection (●).

It would be interesting to compute a transient heat transfer by natural convection from a vertical cylinder placed in an aquifer. Assuming the following physical properties of the aquifer and the cylinder dimensions: $\alpha = 10^{-6}$ m^2 s^{-1}, $\nu = 10^{-7}$ m^2 s^{-1}, $\sigma = 1$, $k_e = 2$ W m^{-1} °C^{-1}, $K = 10^{-10}$ m^2, $a = 0.05$ m, $L = 1$ m, $\Delta T = 10$°C, the corresponding non-dimensional parameters become $Ra_L \cong 10$, $\xi \cong 6$. The resulting average heat transfer coefficient from the cylinder at steady state is about 4.6 W m^{-2} °C^{-1}. Referring to Fig. 5, the time required to reach steady state is about 38 h.

In summary one has found that regardless of forced and natural convection the transient heat transfer from the isothermal cylinder with flows parallel to its axis is dominated by radial heat conduction during a short time. The transitional dimensionless time from the conduction to the convective steady state is proportional to ζ^2 in forced convection and to ξ^2 in natural convection, respectively. For a given cylinder height L/a a vigorous flow generally shortens the time to reach steady state, while for a given flow the greater height lengthens the time.

Acknowledgement—Computer time provided by the Agency of Industrial Science and Technology through its computer network (the Research Information and Processing System) is greatly appreciated.

REFERENCES

1. H. Schlichting, *Boundary-layer Theory*. McGraw-Hill, New York (1968).
2. J. D. Gabor, Heat transfer to particle beds with gas flows less than or equal to that required for incipient fluidization, *Chem. Engng Sci.* **25**, 979–984 (1970).
3. S. Kimura, Forced convection heat transfer about a cylinder placed in a porous medium with longitudinal flows, *Int. J. Heat Fluid Flow* **9**, 83–86 (1988).
4. W. J. Minkowycz and P. Cheng, Free convection about a vertical cylinder embedded in a porous medium, *Int. J. Heat Mass Transfer* **19**, 805–813 (1976).
5. A. Nakayama and H. Koyama, A general similarity transformation for combined free and forced-convection flows within a fluid-saturated porous medium, *J. Heat Transfer* **109**, 1041–1045 (1987).
6. J. H. Merkin, Free convection boundary layers on axisymmetric and two-dimensional bodies of arbitrary shape in a saturated porous medium, *Int. J. Heat Mass Transfer* **22**, 1461–1462 (1979).
7. A. Bejan, Natural convection in an infinite porous medium with a concentrated heat source, *J. Fluid Mech.* **89**, 97–107 (1978).
8. I. Pop and P. Cheng, The growth of a thermal layer in a porous medium adjacent to a suddenly heated semi-infinite horizontal surface, *Int. J. Heat Mass Transfer* **26**, 1574–1576 (1983).
9. H. S. Carslaw and J. C. Jaeger, *Conduction of Heat in Solids*. Clarendon Press, Oxford (1984).
10. A. Bejan, *Convection Heat Transfer*. Wiley, New York (1984).

Int. J. Heat Mass Transfer. Vol. 32, No. 3, pp. 620–624, 1989
Printed in Great Britain

0017 9310/89 $3.00 + 0.00

Evaluation of flux models for radiative transfer in cylindrical furnaces

NEVIN SELÇUK
Department of Chemical Engineering, Middle East Technical University, Ankara 06531, Turkey

(*Received* 17 *March* 1988 *and in final form* 11 *July* 1988)

1. INTRODUCTION

IN A PREVIOUS paper [1], the accuracy of several flux-type models for three-dimensional radiative heat transfer has been assessed by applying these radiation models to the prediction of distributions of the radiative flux density and the radiative energy source term of a rectangular enclosure problem and by comparing their predictions with exact solutions produced earlier by the same author [2]. The problem was based on data taken from a large-scale experimental furnace with steep temperature gradients typical of operating furnaces.

A significant number of industrial furnaces and combustors are cylindrical in shape. Therefore, it is considered necessary to evaluate the flux-type models produced earlier for cylindrical furnaces [3–5] by applying them to the prediction of radiative flux density and source term distributions of a cylindrical enclosure problem based on data reported previously on a pilot-scale experimental furnace [6] and by comparing their predictions with the exact values reported previously [7].

The radiation models to be evaluated are given below.

(1) A Schuster–Hamaker type four-flux model for an axi-symmetrical radiation field derived by Lockwood and Spalding [3].

(2) A Schuster–Schwarzschild type four-flux model derived by Siddall and Selçuk [4].

(3) A Schuster–Schwarzschild type four-flux model produced by Richter and Quack [5].

All these models had previously been employed as part of